Radiology

Nonenhanced MR Angiography of the Hand with Flow-Sensitive Dephasing–prepared Balanced SSFP Sequence: Initial Experience with Systemic Sclerosis[1]

John J. Sheehan, MD
Zhaoyang Fan, PhD[2]
Amir H. Davarpanah, MD
Philip A. Hodnett, MD
John Varga, MD
James C. Carr, MD
Debiao Li, PhD[2]

Purpose: To compare the image quality and degree of vessel narrowing at flow-sensitive dephasing (FSD) magnetic resonance (MR) angiography of the hands with those at contrast material–enhanced MR angiography of the hands in patients with systemic sclerosis.

Materials and Methods: In a single-center study with institutional review board approval and HIPAA compliance, six healthy volunteers and six patients with systemic sclerosis were imaged at 1.5-T nonenhanced FSD MR angiography followed by contrast-enhanced MR angiography. Sixteen vascular segments in four vessel groups were evaluated for image quality and assessed semiquantitatively for stenosis degree by using Likert scales. The nonparametric Wilcoxon signed rank test was used to perform pairwise comparisons of the MR angiographic techniques. $P < .05$ indicated statistical significance.

Results: Performing FSD MR angiography, as compared with time-resolved MR angiography and high-spatial-resolution MR angiography, improved the image quality for all arterial segments combined in the control (mean score, 2.9 [FSD] vs 3.7 [time-resolved technique] and 3.1 [high-spatial-resolution technique]) and patient (mean score, 4.0 [FSD] vs 4.2 [time-resolved technique] and 4.3 [high-spatial-resolution technique]) groups. In the control subjects, FSD angiography depicted proper digital artery stenosis that was less severe (mean grade, 0.7) than that seen with the time-resolved (mean grade, 1.6) and high-spatial-resolution (mean grade, 1.0) techniques. In the patient group, FSD angiography depicted lower degrees of stenosis, with a lower mean grade for all segments combined (1.3) compared with the corresponding mean grades for time-resolved (1.5) and high-spatial-resolution (1.8) MR angiography.

Conclusion: Preliminary data indicate that the proposed nonenhanced FSD MR angiographic technique is an improvement over existing contrast-enhanced techniques for evaluation of the hand vasculature in vasospastic disorders of the hand. Further technical improvements and a systematic clinical study are warranted.

[1] From the Division of Cardiovascular Imaging, Northwestern Memorial Hospital, 737 N Michigan Ave, Suite 1600, Chicago, IL 60611 (J.J.S., P.A.H., J.C.C.); and Departments of Radiology and Biomedical Engineering (Z.F., D.L.), Division of Cardiovascular Imaging (J.J.S., A.H.D., P.A.H., J.C.C.), and Division of Rheumatology, Feinberg School of Medicine (J.V.), Northwestern University, Chicago, Ill.
Received May 9, 2010; revision requested June 15; revision received November 7; accepted November 11; final version accepted November 15. Supported by the National Institutes of Health (grant IR01HL096119).
Address correspondence to J.J.S., Division of Radiology, Hermitage Medical Clinic, Old Lucan Rd, Dublin 20, Ireland (e-mail: *jsheehan@hermitageclinic.ie*).
[2] **Current address:** Division of Radiology and Biomedical Engineering, Cedars-Sinai Medical Center, University of California, Los Angeles, Calif.

Systemic sclerosis is an autoimmune disorder characterized by vasculopathies, including Reynaud phenomenon, which is an early nonspecific set of vasoconstrictive symptoms affecting predominantly the hands and fingers bilaterally (1–3). The diagnosis of Reynaud phenomenon is largely based on the clinical presentation and can be confirmed at angiography. The results of invasive digital subtraction angiography with vasodilators, the standard of reference, have shown that the lesions are found primarily in the proper digital arteries and less frequently in the common digital arteries, deep and superficial arches, and finally ulnar and radial arches (4–7).

Magnetic resonance (MR) angiographic techniques involving the use of gadolinium-based contrast material have become safe and reliable alternatives to digital subtraction angiography (7,8). Evaluation of the hand with MR angiography presents several challenges: First, vessels in the hand are of much smaller caliber than are vessels in the lower extremities and remainder of the body, necessitating higher-spatial-resolution techniques. Second, because arterial and venous collateral vessels are more commonly encountered and the vascular anatomy is much more variable in the hand, the resultant images are difficult to interpret (9). The goals of rapid imaging are the acquisition of a purely arterial image and the minimization of overlap with enhancing veins (9).

Initially, nonenhanced techniques for direct imaging of the hand and wrist vessels with use of two-dimensional time-of-flight sequences were developed (8,10–13). Nonenhanced MR angiographic techniques were subsequently superseded by gadolinium-enhanced MR angiography for applications in the main body and lower extremities owing to the shorter imaging times and decreased motion artifacts with the latter procedure (14–17). A preliminary technique for contrast material–enhanced MR angiography of the hand was described by Rofsky (8). Three-dimensional contrast-enhanced MR angiography is increasingly being performed in patients with Reynaud phenomenon (18–21). Nonenhanced MR angiographic strategies involving the use of three-dimensional half-Fourier fast spin-echo (22) or balanced steady-state free precession (SSFP) (23) sequences have shown great promise, but various challenges remain.

The flow-sensitive dephasing (FSD) MR angiographic technique does not rely on the inflow effect and enables arterial visualization with high isotropic spatial resolution and excellent contrast between arteries and surrounding veins and tissues without use of contrast material. Therefore, it may be suited for imaging tortuous and small hand arteries with substantially slow flow. Similar to fresh blood imaging, FSD MR angiography also requires systolic and diastolic blood flow measurements. During systole, the dark-artery data set is collected because there is a marked difference in velocity between arterial flow and venous flow and an FSD preparation with appropriate gradient strength can induce sufficient intravoxel phase dispersion among arterial spins and thus signal the suppression of arterial blood while having minimal effects on the venous blood and static tissues. During diastole, the bright-artery data set is acquired when arterial flow is substantially slow and the blood signal is bright owing to a T2 preparation (24). Magnitude subtraction of the two image sets permits visualization of arteries, with the background and the venous signals dramatically suppressed. The purpose of this study was to compare the image quality and degree of vessel narrowing seen with a recently introduced nonenhanced MR angiographic technique based on FSD-prepared balanced SSFP with the image quality and degree of vessel narrowing seen with contrast-enhanced MR angiography.

Advance in Knowledge

- Use of nonenhanced flow-sensitive dephasing (FSD) MR angiography resulted in image quality that was similar to that of contrast-enhanced MR angiography for the evaluation of arteries in the hands.

Implication for Patient Care

- FSD-prepared nonenhanced MR angiography of the hands is a noninvasive means of evaluating arterial disease in patients with systemic sclerosis without gadolinium-based contrast material.

Materials and Methods

Subjects

This was a single-center study performed from September 2008 to March 2009. Six healthy volunteers (two men, four women; mean age, 34 years ± 17 [standard deviation]; age range, 24–65 years) were imaged with institutional review board approval and Health Insurance Portability and Accountability Act compliance after they provided written informed consent. Six consecutive patients—three men aged 34–42 years (mean age, 39 years ± 4) and three women aged 38–55 years (mean age, 46 years ± 9)—who were referred for clinical evaluation for known systemic sclerosis were examined with MR angiography. Their medical and imaging data were reviewed with retrospective institutional review board approval and Health Insurance Portability and Accountability Act compliance. Patient inclusion

Published online before print
10.1148/radiol.10100851

Radiology 2011; 259:248–256

Abbreviations:
FSD = flow-sensitive dephasing
SSFP = steady-state free precession

Author contributions:
Guarantors of integrity of entire study, J.J.S., Z.F., D.L.; study concepts/study design or data acquisition or data analysis/interpretation, all authors; manuscript drafting or manuscript revision for important intellectual content, all authors; manuscript final version approval, all authors; literature research, J.J.S., Z.F., A.H.D., P.A.H.; clinical studies, J.J.S., Z.F., P.A.H., J.C.C.; statistical analysis, J.J.S., A.H.D., J.C.C.; and manuscript editing, J.J.S., Z.F., A.H.D., J.V., J.C.C., D.L.

Funding:
This research was supported by the National Institutes of Health (grant 1R01HL096119).

Potential conflicts of interest are listed at the end of this article.

criteria were clinical manifestations of systemic sclerosis and positive autoantibodies. Exclusion criteria were contraindications to MR imaging and an estimated glomerular filtration rate lower than 30 mL/min/1.73 m^2. No patients were excluded from the study.

Imaging Protocol

The healthy control subjects were imaged by using a 1.5-T research MR unit (Espree; Siemens Medical Solutions, Erlangen, Germany). The patients were imaged by using a 1.5-T clinical MR unit (Avanto; Siemens Medical Solutions). Subjects were positioned prone, with their hands over their head in a neutral position and with their palms down. The fingers were spread slightly to prevent overlap of the digital arteries. Two six-channel phased-array body coils (Siemens Medical Solutions) were placed on both sides of the hands to achieve optimal coverage. Electrocardiographic electrodes were attached to the hands to trigger data acquisition. The imaging protocol consisted of FSD followed by contrast-enhanced time-resolved MR angiography and high-spatial-resolution MR angiography of the hands.

FSD-prepared MR angiography.— Phase-contrast flow imaging was performed to derive the arterial flow peak time. Subtraction MR angiography with FSD-prepared balanced SSFP was subsequently conducted and entailed the acquisition of a dark-artery image (Fig 1a) with a trigger delay time and a bright-artery image (Fig 1b) acquired at mid-diastole. FSD gradient pulses were applied in the readout and phase-encoding directions during the dark-artery acquisition for in-plane flow suppression. The first-order gradient moment, m_1, is a measure of the flow sensitization imparted by the FSD preparation (25). In the volunteer studies, the m_1 typically used was approximately 90 mT · $msec^2$/m in either of the two directions. However, when insufficient arterial enhancement or venous overlay occurred, MR angiography was repeated with an m_1 of lower (eg, 60 mT · $msec^2$/m) or higher (up to 110 mT · $msec^2$/m) value. In the patient studies, a constant m_1 was used—100 mT · $msec^2$/m—owing to the imaging time restraint. The balanced SSFP readout parameters included 3.1–3.9/1.5–1.7 (repetition time msec/echo time msec), coronal acquisition, centric view ordering in the phase-encoding direction and linear view ordering in the partition-encoding direction, three shots per partition, 60 segments per shot, a field of view of (316–330) × (316–330) mm, a matrix of 336 × 336, 56–72 sections of 0.94–0.98-mm thickness, spectral-selective fat saturation, a bandwidth of 700–825 Hz/pixel, a generalized autocalibrating partially parallel acquisition imaging factor of two to three, a flip angle of 80°–90°, and an acquisition time of approximately 2–3 minutes per image, depending on the heart rate.

Contrast-enhanced MR angiography.— The protocol for contrast-enhanced MR angiography consisted of time-resolved and high-spatial-resolution MR angiographic examinations after the administration of gadopentetate dimeglumine (Magnevist; Bayer, Berlin, Germany). Time-resolved coronal images were obtained through the hand and wrist by using a multiphase time-resolved angiography with interleaved stochastic trajectories (TWIST) acquisition, with 0.05 mmol of gadopentetate dimeglumine per kilogram of body weight injected at 4 mL/sec followed by a saline flush injected at 8 mL/sec and 4 mL/sec (3.0 seconds per phase, 24 phases starting immediately after contrast material injection). The following parameters were used: 2.7/1.3, a flip angle of 25°, a field of view of 316 × 316 mm, a matrix of 184 × 256 (in-plane spatial resolution, 1.7 × 1.2 mm), 26 sections of 2-mm thickness interpolated to 52 sections of 1-mm thickness, phase partial Fourier factor of 6/8, section partial Fourier factor of 6/8, a bandwidth of 780 Hz/pixel, and a generalized autocalibrating partially parallel acquisition imaging factor of two.

For the high-spatial-resolution MR angiogram acquisitions, 0.15 mmol/kg gadopentetate dimeglumine was injected at 2 mL/sec and followed by a saline flush injected at 20 mL/sec and 2 mL/sec. Three measurement acquisitions were

Figure 1

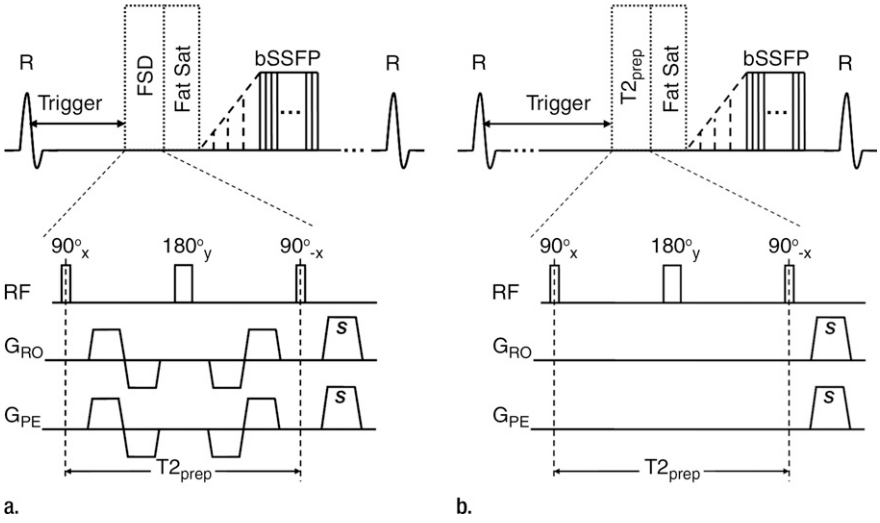

Figure 1: Sequence diagrams illustrate **(a)** dark-artery MR angiography procedure, with FSD-prepared balanced SSFP *(bSSFP)* triggered at systole and **(b)** bright-artery MR angiography procedure, with T2-prepared *($T2_{prep}$)* balanced SSFP triggered at diastole. Both FSD preparation and T2 preparation consist of 90°*x*-180°*y*-90°*x* radiofrequency *(RF)* series and are of the same duration to maintain the same T2 weighting for venous blood and static tissues. FSD gradient pulse applied in readout direction *(G_{RO})* and FSD gradient pulse applied in phase-encoding direction *(G_{PE})* are simultaneously switched on in FSD preparation but switched off in T2 preparation. Readout direction coincides with main blood flow direction. FSD or T2 preparation is followed by a spectrally selective fat-saturation *(Fat Sat)* radiofrequency module and 10 preparation radiofrequency pulses with linearly increasing flip angles before the balanced SSFP data acquisition. *R* = R wave, *s* = sample.

Segments That Demonstrated Nondiagnostic Arterial Display with the Three MR Angiographic Techniques

Segments and Subject Groups	FSD*	TR*	HR*	*P* Value		
				FSD vs TR	FSD vs HR	TR vs HR
Control subjects						
Proper digital arterial segments	14 (7.3)	52 (27.1)	24 (12.5)	<.001†	.06	<.001†
Ulna-radius, arch, and common digital arterial segments	14 (7.3)	58 (30.2)	25 (13.0)	<.001†	.05	<.001†
Patients						
Proper digital arterial segments	58 (33.0)	60 (34.1)	50 (28.4)	.68	.17	.06
Ulna-radius, arch, and common digital arterial segments	85 (48.3)	93 (52.8)	92 (52.3)	.18	.38	>.99

Note.—HR = high-spatial-resolution MR angiography, TR = time-resolved MR angiography.

* Data are numbers of segments that demonstrated nondiagnostic arterial display. Numbers in parentheses are percentages based on totals of 192 segments in the control group and 176 segments in the patient group.

† Significant difference between given MR angiographic techniques.

performed: The first acquisition was performed before the contrast material injection, and the second and third acquisitions were performed continuously, after a waiting period following the contrast material administration, the timing of which was determined according to the TWIST results (20–36 seconds), with each measurement lasting 22 seconds. The following parameters were used: 3.3/1.2, a field of view of 315 × 360 mm, a matrix of 336 × 384, 56 sections of 0.94-mm thickness (isotropic spatial resolution, 0.94 × 0.94 × 0.94 mm), a flip angle of 25°, a time to center of 7.8 seconds, a phase partial Fourier factor of 6/8, a section partial Fourier factor of 6/8, a bandwidth of 565 Hz/pixel, and a generalized autocalibrating partially parallel acquisition imaging factor of two. The subtracted images were processed by using a maximum intensity projection for interpretation.

Image Analysis

The images obtained by using each MR angiographic protocol were analyzed by two radiologists (J.J.S., P.A.H., 5 and 2 years experience, respectively, in MR angiogram interpretation) in consensus at a workstation (Leonardo; Siemens Medical Solutions). The readings were spaced 2 weeks apart. Sixteen vascular segments were evaluated: ulnar segment, radial segment, superficial arch, deep arch, three common digital arteries, and nine proper digital arteries. The segments were subsequently grouped into four region groups: ulna and radius, arches, common digital arteries, and proper digital arteries.

The image quality of the angiograms obtained in both subject groups was assessed by using a five-point Likert scale: A score of 1 indicated excellent arterial diagnostic display and differentiation of the arterial vasculature from the background tissue; a score of 2, good diagnostic arterial display without impaired delineation of the vessel structures; a score of 3, fair diagnostic arterial display and delineation of the arterial structures, with exclusion and detection of lesions still possible; a score of 4, poor diagnostic arterial display with inadequate vessel enhancement or severe blurring; and a score of 5, nondiagnostic arterial display (26).

The degree of stenosis was semiquantitatively assessed by using a three-point scale for the control group—grade 0 indicated normal patency; grade 1, apparent narrowing; and grade 2, nonvisualization—and by using a four-point scale for the patient group—grade 0 indicated normal patency; grade 1, less than or equal to 50% luminal narrowing; grade 2, greater than or equal to 51% luminal narrowing; and grade 3, occlusion (26). When two or more stenoses were present in one segment, the most severe lesion was used for the subsequent assignment of a grade. The presence of digital arteries visualized to the distal third was recorded for both groups.

Statistical Analyses

SPSS, version 17.0 (SPSS, Chicago Ill), software was used to perform the statistical analyses. Scores were calculated by comparing the mean image quality and stenosis degree scores for each segment and the four regions (ulna and radius, superficial and deep arches, common digital arteries, proper digital arteries) obtained with the FSD, contrast-enhanced time-resolved, and contrast-enhanced high-spatial-resolution MR angiographic techniques. The nonparametric Wilcoxon signed rank test was used to perform pairwise comparisons of the segments, regions, and overall quality scores with each MR angiographic technique. $P < .05$ was considered to indicate a statistically significant difference. All results were expressed as means. To compare the number of distal digital arteries visualized as well as the prevalence of nondiagnostic segments between the MR angiographic techniques, the McNemar exact test was used.

Results

There were 192 and 176 segments in the control and patient groups, respectively. One patient was unable to lie with both hands in the imaging plane, so only one hand was imaged. The mean qualitative and semiquantitative scores for FSD angiography, time-resolved MR angiography, and high-spatial-resolution MR angiography in the control and patient groups are summarized in Figure 2. Nondiagnostic display of the arterial segments was demonstrated in both the control group and the patient group with all three angiographic techniques and involved predominantly the proper digital arteries (Table).

Image Quality

In the control group, mean image quality scores for all segments and regions

Figure 2

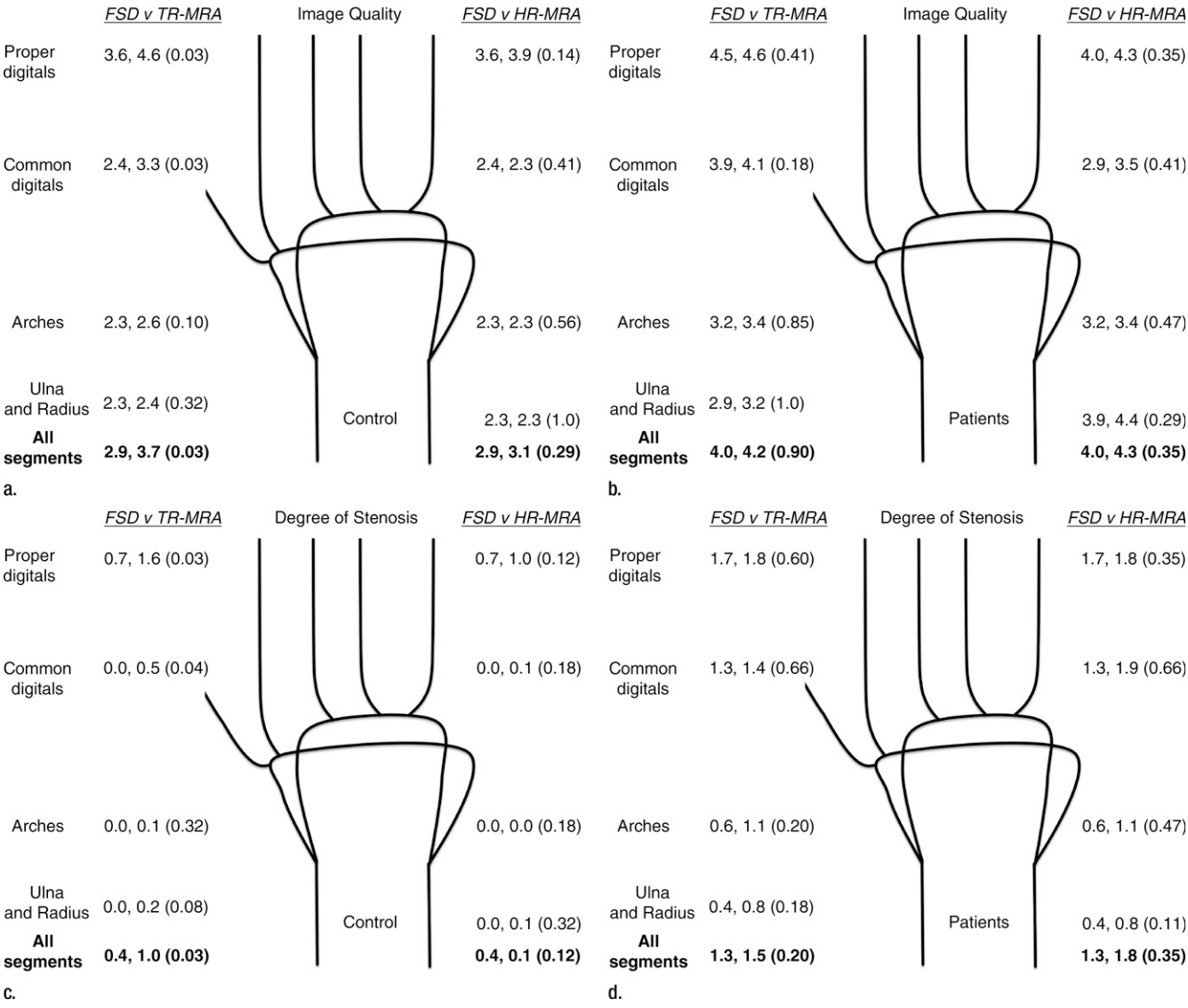

Figure 2: Mean qualitative (image quality) and semiquantitative (stenosis degree) scores for nonenhanced FSD MR angiography, as compared with contrast-enhanced time-resolved *(TR-MRA)* or high-spatial-resolution *(HR-MRA)* MR angiography, with corresponding schematics of hand arteries. Lower mean image quality scores correlate with improved image quality. Higher mean stenosis degree scores correlate with increased apparent degree of stenosis. Mean image quality scores for the **(a)** control subjects and **(b)** patients and mean stenosis degree scores for the **(c)** control subjects and **(d)** patients are compared between the angiographic techniques. In each set of numbers, first value is mean score with FSD, second number is mean score with time-resolved or high-spatial-resolution MR angiography, and number in parentheses is *P* value for given comparison.

with FSD, as compared with time-resolved MR angiography, were improved and were significantly different for all segments combined and in the regions of the common digital and proper digital arteries. The mean image quality scores with FSD, as compared with high-spatial-resolution MR angiography, were improved for all segments combined. Mean scores were equal in the regions of the ulnar and radius and the arches (2.3 for FSD and high-spatial-resolution techniques in both regions) and slightly lower than those in the common digital artery region (2.4, 2.3) (Figs 2, 3).

In the patient group, mean image quality scores for all segments and regions with FSD, as compared with both contrast-enhanced MR angiographic techniques, were improved but not significantly different (Fig 4). With all three techniques, the image quality was lower in all categories compared with the image quality in the control group (mean scores with FSD: 4.0 for patients, 2.9 for control subjects). Mean scores worsened in proportion to the distal

Figure 3

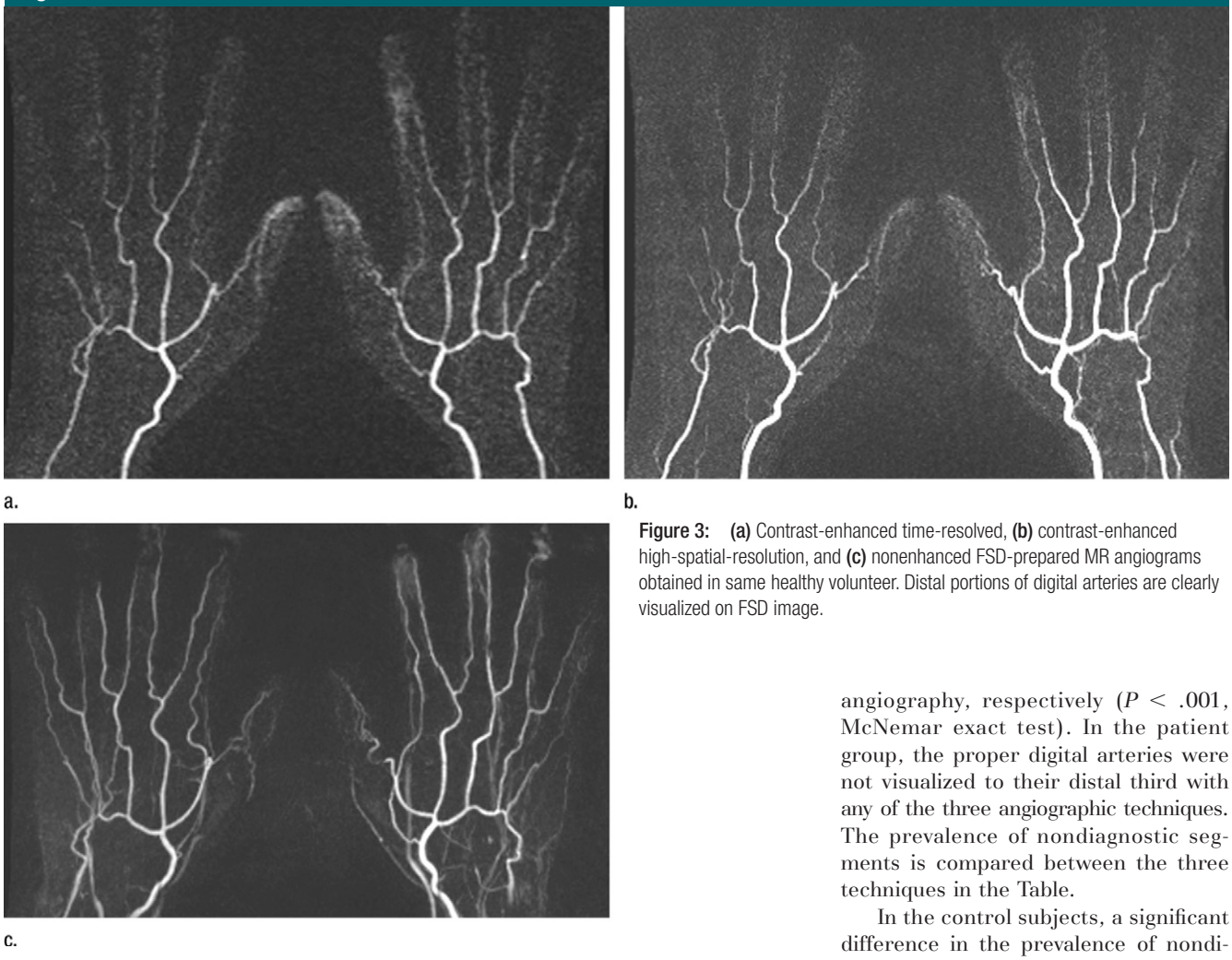

Figure 3: **(a)** Contrast-enhanced time-resolved, **(b)** contrast-enhanced high-spatial-resolution, and **(c)** nonenhanced FSD-prepared MR angiograms obtained in same healthy volunteer. Distal portions of digital arteries are clearly visualized on FSD image.

extent of the region (mean scores with FSD: 2.9, 3.2, 3.9, and 4.5 for ulna and radius, arches, common digital arteries, and proper digital arteries, respectively).

Stenosis

In the evaluation of the degree of apparent stenosis in the control group, FSD angiography depicted no stenosis in the ulna and radius, arches, or common digital arteries. FSD images depicted apparent stenosis in the proper digital arteries, however, with a mean stenosis degree grade of 0.7, which was lower than the mean stenosis degree grades with the time-resolved (grade, 1.6) and high-spatial-resolution (grade, 1.0) MR angiographic techniques. The differences in mean grades between FSD and time-resolved MR angiography were significant for all segments combined and all regions except the arches.

In the evaluation of the degree of stenosis in the patient group, FSD angiography, as compared with both contrast-enhanced MR angiographic techniques, depicted lower degrees of stenosis, with lower mean grades for all segments combined and all regions. However, the differences were not significant.

In the control group, 50 (79%) of the 63 digital arteries were visualized to their distal third with FSD compared with three (5%) and 13 (21%) digital arteries that were visualized to this extent with time-resolved MR angiography and high-spatial-resolution MR angiography, respectively ($P < .001$, McNemar exact test). In the patient group, the proper digital arteries were not visualized to their distal third with any of the three angiographic techniques. The prevalence of nondiagnostic segments is compared between the three techniques in the Table.

In the control subjects, a significant difference in the prevalence of nondiagnostic segments between the FSD, time-resolved, and high-spatial-resolution MR angiographic techniques was noted ($P < .05$ for all comparisons). When the comparison was limited to the distal digital vessels, a significant difference was seen between FSD and time-resolved MR angiography ($P < .05$) and between time-resolved and high-spatial-resolution MR angiography ($P < .05$) only, and the 28 additional nondiagnostic segments seen with time-resolved MR angiography, as compared with FSD, did not constitute a significant difference ($P = .06$). In the patients, the difference in the prevalence of nondiagnostic segments between the MR angiographic techniques failed to reach significance ($P > .05$, McNemar exact test).

Figure 4

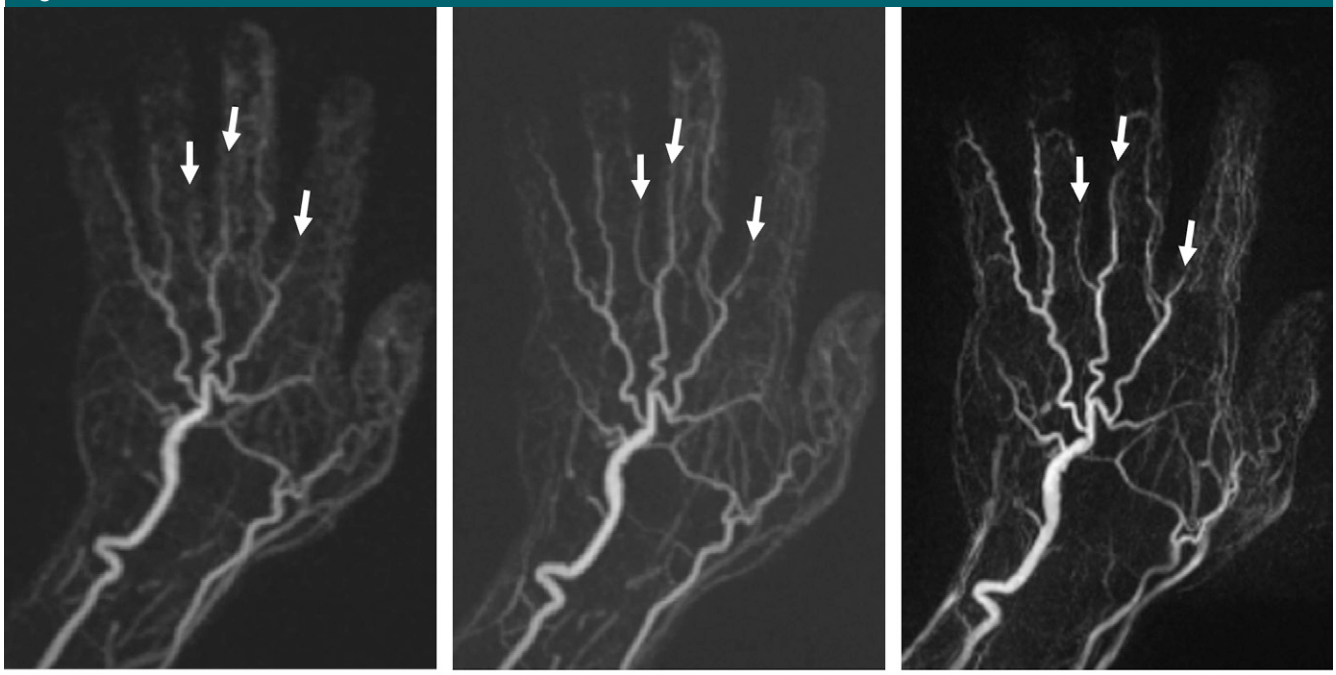

a. b. c.

Figure 4: **(a)** Contrast-enhanced time-resolved, **(b)** contrast-enhanced high-spatial-resolution, and **(c)** nonenhanced FSD-prepared MR angiograms obtained in patient with focal mild stenosis (arrows) involving proper digital arteries of index, middle, and ring fingers of left hand.

Discussion

In the described initial applications in the hand, the FSD technique, based on segmented balanced SSFP and involving a combination of electrocardiographic triggering, FSD magnetization preparation, and subtraction techniques, was compared with contrast-enhanced MR angiography. Isotropic submillimeter-spatial-resolution angiograms with bright arterial blood and suppressed background were successfully obtained in healthy volunteers and patients with systemic sclerosis.

Our pilot study results show that FSD angiography, as compared with contrast-enhanced MR angiography, yields similar mean qualitative and semiquantitative scores in control and patient groups. Overall, the mean scores for image quality and degree of apparent or true stenosis favored FSD over both contrast-enhanced angiographic techniques—particularly at comparison of FSD angiography and time-resolved MR angiography, where the differences were significant in the majority cases. However, while the observed lower degrees of stenoses suggest that FSD findings may be more accurate determinants of vessel diameter, this theory was not adequately assessed in this study and no reference-standard digital subtraction angiographic examination was performed to confirm it. When the proper digital arteries in the healthy control group were identified—in the majority of cases—the three MR angiographic techniques revealed varying degrees of apparent stenosis. This finding highlights one of the limitations of MR angiography in the evaluation of very-small-diameter vessels.

A link between the use of gadolinium-containing contrast agents in patients with end-stage renal disease and a rare and debilitating condition referred to as nephrogenic systemic fibrosis has been established (27) and has led to a renaissance of the use of nonenhanced MR angiographic techniques over the past few years. With nonenhanced MR angiographic techniques, one always has the option to repeat all or part of the data acquisition in cases of technical difficulty or patient motion—an option not afforded by contrast-enhanced MR angiography. Moreover, for patients with an estimated glomerular filtration rate higher than 30 mL/min/1.73 m^2, the nonenhanced MR angiographic examination can be following by a contrast-enhanced study if the image quality for one or more segments is deemed unsatisfactory. In addition, nonenhanced MR angiography can be repeated before and after the administration of vasoactive drugs or cold stimuli to study changes in the arterial system.

Several advantages of the FSD technique over other nonenhanced MR angiographic methods are detailed in a previous work (25) and include isotropic high spatial resolution and a sufficiently clean background, which may favor visualization of the relatively tortuous small-caliber arterial anatomy in the hand. Fresh blood imaging is a subtraction technique that involves a three-dimensional half-Fourier fast spin-echo pulse sequence in conjunction with selective application of flow-spoiling gradients to ensure that the rapidly flowing arterial spins are fully suppressed (22).

This technique requires calibration of the trigger delay and flow-spoiling gradients for individual patients and vessel segments. The major advantage of using the fresh blood imaging technique is that it is independent of the inflow of fresh blood into the imaging volume. Therefore, it can be used to image arteries with relatively slow flow, such as those in the hand. However, long-echo-train fast spin-echo acquisitions are inherently susceptible to fast and complex flow at and distal to stenoses and thereby result in loss of the flow signal on images acquired without flow-spoiling gradients. It is worthwhile to compare FSD angiography with fresh blood imaging, as these techniques have several technical aspects in common, including flow spoiling, systolic and diastolic acquisitions, and subtraction (22). The described FSD technique involves a balanced SSFP acquisition in conjunction with an independent flow-suppression preparation module (25). Compared with a long-echo fast spin-echo sequence, as is used in fresh blood imaging, balanced SSFP imaging without FSD gradient pulses may depict brighter arterial blood owing to lower sensitivity to flow and the high T2/T1 ratio of blood (28). With a separate flow-suppression preparation module, the FSD gradient pulses can be flexibly configured in both direction and strength such that multidirectional flow suppression in the hand is feasible. However, this flexibility is not inherent to the fresh blood imaging sequence.

This recently introduced FSD technique has a number of drawbacks. First, it requires long imaging times owing to electrocardiographic triggering and separate sequential imaging during systole and diastole, so it is more prone to motion artifacts. This may be problematic in hand studies if the patient is not comfortable in the prone position. Second, balanced SSFP images may be corrupted by pronounced off-resonance artifacts that occur owing to magnetic induction field inhomogeneity and susceptibility effects, which were noted in the wrist in our studies.

There were several limitations of our study. First, digital subtraction angiography was not available for correlation. Second, the patient data analysis was semiquantitative, so we did not quantify vessel diameters and stenosis lengths. Third, the control subjects and patients were imaged with different 1.5-T MR units. Fourth, one cannot assume that the imaging parameters found to be optimal in this initial study will prove to be best for all subjects. Fifth, we did not use any arterial cuff compression techniques to perform the described contrast-enhanced MR angiography examination described herein (29,30). Sixth, the study sample was small. Finally, it should be recognized that contrast-enhanced MR angiography offers certain advantages over current nonenhanced methods, such as shorter imaging times and the ability to acquire time-resolved images that show blood flow dynamics.

More experience with nonenhanced and contrast-enhanced MR angiography of the hand is required to establish the accuracy of these examinations, as compared with that of digital subtraction angiography, the reference standard. Allanore et al (18) suggest that MR angiography could be used to predict end-stage ischemic damage in the fingers and other organs, because hand vessel lesions may reflect general vasculopathy. Cross-sectional studies to correlate MR angiographic findings with biochemical and clinical parameters of the hand and pulmonary vasculature are needed. Furthermore, longitudinal studies could be used to evaluate MR angiographic findings as predictors of ulceration, pulmonary hypertension, and responses to aggravating factors and therapy.

Nonenhanced FSD MR angiograms of the hand that depict normal and diseased segments can be generated. In control subjects and patients with systemic sclerosis, FSD angiography compares favorably with contrast-enhanced MR angiography, facilitating improved visualization of normal and diseased vessels in many cases. Nevertheless, this technique needs further technical improvements and to be evaluated in a systematic clinical study to clarify its diagnostic accuracy.

Disclosures of Potential Conflicts of Interest: J.J.S. Financial activities related to the present article: received a grant from the National Institutes of Health. Financial activities not related to the present article: none to disclose. Other relationships: none to disclose. **Z.F.** Financial activities related to the present article: received a grant from the National Institutes of Health. Financial activities not related to the present article: none to disclose. Other relationships: none to disclose. **A.H.D.** No potential conflicts of interest to disclose. **P.A.H.** No potential conflicts of interest to disclose. **J.V.** No potential conflicts of interest to disclose. **J.C.C.** Financial activities related to the present article: none to disclose. Financial activities not related to the present article: received a grant or grants are pending from Siemens Medical Solutions. Other relationships: none to disclose. **D.L.** No potential conflicts of interest to disclose.

References

1. Campbell PM, LeRoy EC. Pathogenesis of systemic sclerosis: a vascular hypothesis. Semin Arthritis Rheum 1975;4(4):351–368.
2. D'Angelo WA, Fries JF, Masi AT, Shulman LE. Pathologic observations in systemic sclerosis (scleroderma): a study of fifty-eight autopsy cases and fifty-eight matched controls. Am J Med 1969;46(3):428–440.
3. Herrick AL. Vascular function in systemic sclerosis. Curr Opin Rheumatol 2000;12(6):527–533.
4. Dabich L, Bookstein JJ, Zweifler A, Zarafonetis CJ. Digital arteries in patients with scleroderma: arteriographic and plethysmographic study. Arch Intern Med 1972;130(5):708–714.
5. Janevski B. Arteries of the hand in patients with scleroderma. Diagn Imaging Clin Med 1986;55(4-5):262–265.
6. Loring LA, Hallisey MJ. Arteriography and interventional therapy for diseases of the hand. RadioGraphics 1995;15(6):1299–1310.
7. Lee VS, Lee HM, Rofsky NM. Magnetic resonance angiography of the hand: a review. Invest Radiol 1998;33(9):687–698.
8. Rofsky NM. MR angiography of the hand and wrist. Magn Reson Imaging Clin N Am 1995;3(2):345–359.
9. Goldfarb JW, Hochman MG, Kim DS, Edelman RR. Contrast-enhanced MR angiography and perfusion imaging of the hand. AJR Am J Roentgenol 2001;177(5):1177–1182.
10. Disa JJ, Chung KC, Gellad FE, Bickel KD, Wilgis EF. Efficacy of magnetic resonance angiography in the evaluation of vascular malformations of the hand. Plast Reconstr Surg 1997;99(1):136–144; discussion 145–147.
11. Dobson MJ, Hartley RW, Ashleigh R, Watson Y, Hawnaur JM. MR angiography and MR imaging of symptomatic vascular malformations. Clin Radiol 1997;52(8):595–602.

12. Holder LE, Merine DS, Yang A. Nuclear medicine, contrast angiography, and magnetic resonance imaging for evaluating vascular problems in the hand. Hand Clin 1993; 9(1):85–113.

13. Laor T, Burrows PE, Hoffer FA. Magnetic resonance venography of congenital vascular malformations of the extremities. Pediatr Radiol 1996;26(6):371–380.

14. Hany TF, Debatin JF, Leung DA, Pfammatter T. Evaluation of the aortoiliac and renal arteries: comparison of breath-hold, contrast-enhanced, three-dimensional MR angiography with conventional catheter angiography. Radiology 1997;204(2):357–362.

15. Prince MR, Narasimham DL, Stanley JC, et al. Breath-hold gadolinium-enhanced MR angiography of the abdominal aorta and its major branches. Radiology 1995;197(3):785–792.

16. Rofsky NM, Johnson G, Adelman MA, Rosen RJ, Krinsky GA, Weinreb JC. Peripheral vascular disease evaluated with reduced-dose gadolinium-enhanced MR angiography. Radiology 1997;205(1):163–169.

17. Wang Y, Lee HM, Khilnani NM, et al. Bolus-chase MR digital subtraction angiography in the lower extremity. Radiology 1998; 207(1):263–269.

18. Allanore Y, Seror R, Chevrot A, Kahan A, Drapé JL. Hand vascular involvement assessed by magnetic resonance angiography in systemic sclerosis. Arthritis Rheum 2007; 56(8):2747–2754.

19. Wang J, Yarnykh VL, Molitor JA, et al. Micro magnetic resonance angiography of the finger in systemic sclerosis. Rheumatology (Oxford) 2008;47(8):1239–1243.

20. Walcher J, Strecker R, Goldacker S, Winterer J, Langer M, Bley TA. High resolution 3 tesla contrast-enhanced MR angiography of the hands in Raynaud's disease. Clin Rheumatol 2007;26(4):587–589.

21. Connell DA, Koulouris G, Thorn DA, Potter HG. Contrast-enhanced MR angiography of the hand. RadioGraphics 2002;22(3):583–599.

22. Miyazaki M, Takai H, Sugiura S, Wada H, Kuwahara R, Urata J. Peripheral MR angiography: separation of arteries from veins with flow-spoiled gradient pulses in electrocardiography-triggered three-dimensional half-Fourier fast spin-echo imaging. Radiology 2003;227(3):890–896.

23. Stafford RB, Sabati M, Mahallati H, Frayne R. 3D non-contrast-enhanced MR angiography with balanced steady-state free precession Dixon method. Magn Reson Med 2008;59(2):430–433.

24. Shea SM, Deshpande VS, Chung YC, Li D. Three-dimensional true-FISP imaging of the coronary arteries: improved contrast with T2-preparation. J Magn Reson Imaging 2002; 15(5):597–602.

25. Fan Z, Sheehan J, Bi X, Liu X, Carr J, Li D. 3D noncontrast MR angiography of the distal lower extremities using flow-sensitive dephasing (FSD)-prepared balanced SSFP. Magn Reson Med 2009;62(6): 1523–1532.

26. Lim RP, Storey P, Atanasova IP, et al. Three-dimensional electrocardiographically gated variable flip angle FSE imaging for MR angiography of the hands at 3.0 T: initial experience. Radiology 2009;252(3):874–881.

27. Grobner T. Gadolinium: a specific trigger for the development of nephrogenic fibrosing dermopathy and nephrogenic systemic fibrosis? Nephrol Dial Transplant 2006;21(4): 1104–1108. [Published correction appears in Nephrol Dial Transplant 2006;21(6):1745.]

28. Scheffler K, Lehnhardt S. Principles and applications of balanced SSFP techniques. Eur Radiol 2003;13(11):2409–2418.

29. Gluecker TM, Bongartz G, Ledermann HP, Bilecen D. MR angiography of the hand with subsystolic cuff-compression optimization of injection parameters. AJR Am J Roentgenol 2006;187(4):905–910.

30. Wentz KU, Fröhlich JM, von Weymarn C, Patak MA, Jenelten R, Zollikofer CL. High-resolution magnetic resonance angiography of hands with timed arterial compression (tac-MRA). Lancet 2003;361(9351): 49–50.